

# Montane forest productivity across a semiarid climatic gradient

John F. Knowles<sup>1,2</sup>  | Russell L. Scott<sup>1</sup> | Joel A. Biederman<sup>1</sup>  | Peter D. Blanken<sup>3</sup> | Sean P. Burns<sup>3,4</sup> | Sabina Dore<sup>5</sup>  | Thomas E. Kolb<sup>5</sup> | Marcy E. Litvak<sup>6</sup>  | Greg A. Barron-Gafford<sup>2</sup>

<sup>1</sup>Southwest Watershed Research Center, USDA Agricultural Research Service, Tucson, AZ, USA

<sup>2</sup>School of Geography, Development & Environment, University of Arizona, Tucson, AZ, USA

<sup>3</sup>Department of Geography, University of Colorado Boulder, Boulder, CO, USA

<sup>4</sup>National Center for Atmospheric Research, Boulder, CO, USA

<sup>5</sup>School of Forestry, Northern Arizona University, Flagstaff, AZ, USA

<sup>6</sup>Department of Biology, University of New Mexico, Albuquerque, NM, USA

## Correspondence

John F. Knowles, USDA-ARS Southwest Watershed Research Center, 2000 E. Allen Road, Tucson, AZ 85719, USA.  
Email: John.Knowles@usda.gov

## Funding information

U.S. Department of Energy, Grant/Award Number: 7074628 and 7094866; USDA; NSF, Grant/Award Number: EAR-1417101 and EAR-1331408

## Abstract

High-elevation montane forests are disproportionately important to carbon sequestration in semiarid climates where low elevations are dry and characterized by low carbon density ecosystems. However, these ecosystems are increasingly threatened by climate change with seasonal implications for photosynthesis and forest growth. As a result, we leveraged eddy covariance data from six evergreen conifer forest sites in the semiarid western United States to extrapolate the status of carbon sequestration within a framework of projected warming and drying. At colder locations, the seasonal evolution of gross primary productivity (GPP) was characterized by a single broad maximum during the summer that corresponded to snow melt-derived moisture and a transition from winter dormancy to spring activity. Conversely, winter dormancy was transient at warmer locations, and GPP was responsive to both winter and summer precipitation such that two distinct GPP maxima were separated by a period of foresummer drought. This resulted in a predictable sequence of primary limiting factors to GPP beginning with air temperature in winter and proceeding to moisture and leaf area during the summer. Due to counteracting winter (positive) and summer (negative) GPP responses to warming, leaf area index and moisture availability were the best predictors of annual GPP differences across sites. Overall, mean annual GPP was greatest at the warmest site due to persistent vegetation photosynthetic activity throughout the winter. These results indicate that the trajectory of this region's carbon sequestration will be sensitive to reduced or delayed summer precipitation, especially if coupled to snow drought and earlier soil moisture recession, but summer precipitation changes remain highly uncertain. Given the demonstrated potential for seasonally offsetting responses to warming, we project that decadal semiarid montane forest carbon sequestration will remain relatively stable in the absence of severe disturbance.

## KEYWORDS

carbon, dormancy, eddy covariance, evergreen conifer, flux, monsoon, mountain, semi-arid, snow, southwest

## 1 | INTRODUCTION

Temperate forest ecosystems represent an important carbon sink that is currently acting to mitigate global climate change (Griscom et al., 2017; Pan et al., 2011). In semiarid western North America, the majority of carbon sequestration occurs in montane forests where orographic precipitation moderates prevailing moisture limitation to growth (Schimel et al., 2002). In these forests, primary production is regulated by feedbacks between energy, moisture, and disturbance that vary over space and time (Bonan, 2008; Millar & Stephenson, 2015). Western North America is currently experiencing rapid warming and aridification with unknown implications for the regional carbon sink (Harpold et al., 2012; Luce et al., 2016). In semiarid western North America, climate models project a 2.1°C–2.7°C increase in the regional annual average air temperature by mid-century (2036–2065), enhanced winter drying, and increased probability of decadal to multi-decadal megadrought (Ault, Mankin, Cook, & Smerdon, 2016; Jones & Gutzler, 2016; Vose, Easterling, Kunkel, LeGrande, & Wehner, 2017). Although previous studies report negative impacts of climate change on forest growth (Charney et al., 2016; Schwalm et al., 2012; Williams et al., 2013) and/or resilience to disturbance (Davis et al., 2019; Hessburg et al., 2019), ecological change may not manifest equally across the landscape due to broad hydrometeorological gradients that co-occur with elevation, latitude, and proximity to the North American Monsoon (hereafter “monsoon”). As a result, this study investigated a broad climatic gradient to determine how expected climate changes may affect the regional montane forest biome.

The seasonality and type of precipitation impact moisture availability and montane forest carbon sequestration through a variety of mechanisms (e.g., Allen, Kirchner, Braun, Siegwolf, & Goldsmith, 2019; Brooks & Vivoni, 2008). At higher latitude and/or elevation locations that are characterized by consistent seasonal snow cover, the spring snow melt moisture pulse is often sufficient to satisfy the bulk of vegetation water demand throughout the growing season (Hu, Moore, Burns, & Monson, 2010; Knowles, Lestak, & Molotch, 2017; Trujillo, Molotch, Goulden, Kelly, & Bales, 2012). However, recent work has also highlighted the sensitivity of montane forest gross primary productivity (GPP) to summer rain, especially at high elevations or following high snowpack years (Berkelhammer, Stefanescu, Joiner, & Anderson, 2017; Berkelhammer et al., 2020). Under these circumstances, greater sensitivity to summer rain may reflect a longer residence time of precipitation in the root zone when soils are wet or shallower rooting depths when and where precipitation is greater (Fan, Miguez-Macho, Jobbágy, Jackson, & Otero-Casal, 2017; Martin, Looker, Hoylman, Jencso, & Hu, 2018; Szejner et al., 2016). At relatively low latitudes and/or elevations, winter precipitation occurs as both rain and snow, and seasonal snow cover may be ephemeral or inconsistent on an interannual basis (Petersky, Shoemaker, Weisberg, & Harpold, 2019). Without reliable inputs of snow melt-derived moisture, foreshortened droughts occur with greater frequency and severity, and vegetation is dependent on monsoon precipitation to a

greater degree (Peltier & Ogle, 2019; Sloat, Henderson, Lamanna, & Enquist, 2015). Given that the dependence of trees on precipitation inputs varies throughout the year, changes in the seasonality and/or type of precipitation may be experienced differently throughout the montane forest biome.

Growing seasons are lengthening globally with uncertain and uneven implications for vegetation activity (Keeling, Chin, & Whorf, 1996; Reyes-Fox et al., 2014). In the semiarid western United States, there is a growing consensus that longer growing seasons may have a net negative effect on montane forest carbon sequestration as a result of novel interactions between changes in temperature, moisture, and photoperiod (e.g., Boisvenue & Running, 2010; Hu et al., 2010; Knowles, Molotch, Trujillo, & Litvak, 2018; Winchell, Barnard, Monson, Burns, & Molotch, 2016), but the potential for warming to affect winter dormancy in evergreen conifer vegetation remains unclear. Mid-latitude evergreen conifer forests typically experience winter dormancy due to constraints on biological processes imposed by low air temperatures (e.g., Havranek & Tranquellini, 1995). The extent of winter dormancy, however, and the transition from winter dormancy to spring activity, depends on complex interactions between physiological mechanisms and meteorological forcing that can vary among species (Bowling et al., 2018; Nippert, Duursma, & Marshall, 2004). For example, in a high-elevation subalpine forest, frozen tree boles prohibited winter photosynthetic activity even during periods of favorable weather (Bowling et al., 2018), but work from milder sites in the western United States and Europe has suggested that winter photosynthesis can reach 30%–75% of peak growing season rates (Kelly & Goulden, 2016; Knowles, Scott, Minor, & Barron-Gafford, 2020; Potts, Minor, Braun, & Barron-Gafford, 2017; Wieser, 1997). Therefore, a principal objective of the current study was to investigate the effect of longer growing seasons on the seasonality of montane forest GPP at various locations along a semiarid climatic gradient, and to leverage that information to gain insight about future conditions.

The eddy covariance technique is the state-of-the-art approach for measuring ecosystem-atmosphere carbon dioxide exchange (Baldocchi, 2020). Yet, the establishment of eddy covariance sites in mountains has lagged other ecosystem types due to difficulties associated with establishing sites and measuring turbulent fluxes in complex mountain terrain (e.g., Baldocchi, Finnigan, Wilson, Paw, & Falge, 2000; Sun et al., 2010). Recently, additional AmeriFlux sites in the western United States have made it possible to directly compare seasonal GPP from montane forest sites that are subject to distinct air temperature and precipitation regimes (Table 1; Figure 1). Accordingly, the current study assimilated data from six montane forests to project the status of montane forest carbon sequestration under anticipated climatic warming and drying scenarios. We specifically addressed the following research questions: (a) To what degree is the intra-annual GPP distribution modified by differences in air temperature and the seasonality and type of precipitation among sites and years? And, how does this response inform (b) process-based understanding of GPP and (c) current projections

**TABLE 1** Site background information. MAT is mean annual air temperature, MAP is mean annual precipitation, and Snow:rain ratio is based on an air temperature threshold of 0°C. Values in parentheses are standard deviation

Site ID	Site name	Elevation (m)	Dominant species	Observation years	MAT (°C)	MAP (mm)	Snow:rain ratio	Fraction monsoon precipitation	Reference
US-MtB	Mt. Bigelow	2,573	<i>Pinus ponderosa</i> ; <i>Pseudotsuga menziesii</i> ; <i>Pinus strobiformis</i>	2010–2018	10.0	604	0.11 (0.10)	0.46 (0.17)	Knowles et al. (2020)
US-Fuf	Flagstaff unmanaged forest	2,180	<i>P. ponderosa</i>	2005–2010	9.0	562	0.13 (0.08)	0.38 (0.12)	Dore et al. (2008)
US-Vcp	Valles Caldera ponderosa	2,500	<i>P. ponderosa</i> ; <i>Quercus gambelii</i>	2007–2018	7.4	454	0.11 (0.05)	0.34 (0.09)	Anderson-Teixeira et al. (2011)
US-Vcs	Valles Caldera Sulphur Springs mixed conifer	2,752	<i>P. ponderosa</i> ; <i>P. menziesii</i> ; <i>Abies concolor</i> ; <i>Picea pungens</i> ; <i>Populus tremuloides</i>	2016–2018	7.0	620	0.38 (0.19)	0.33 (0.07)	Litvak (2016)
US-Vcm	Valles Caldera mixed conifer	3,030	<i>P. menziesii</i> ; <i>A. concolor</i> ; <i>Abies lasiocarpa</i> ; <i>P. pungens</i> ; <i>P. tremuloides</i>	2007–2013	5.2	661	0.35 (0.12)	0.29 (0.12)	Anderson-Teixeira et al. (2011)
US-NR1	Niwot Ridge	3,050	<i>Pinus contorta</i> ; <i>A. lasiocarpa</i> ; <i>Picea engelmannii</i>	1999–2018	2.4	762	0.61 (0.08)	0.20 (0.08)	Turnipseed et al. (2002)

of semiarid montane forest carbon cycling within the context of forecasted climate changes? We expected to find evidence of trade-offs between early season vegetation greening and late season water deficits as a result of differences in latitude/elevation and seasonal precipitation with implications for annual carbon sequestration.

## 2 | MATERIALS AND METHODS

### 2.1 | Study sites

Figure 1 shows the location of our six montane evergreen conifer forest study sites in the southwestern United States. Here, we define “montane” as “of the mountain” and include both Rocky Mountain and Madrean evergreen conifer forests that populate high plateaus and mountains from Colorado, United States to the Sierra Madre, Mexico (Pase & Brown, 1994). The sites spanned 8 degrees of latitude and 870 m elevation and represented a gradient from cooler conditions with precipitation more evenly distributed throughout the year in the north to warmer conditions with a bimodal precipitation distribution in the south (Figure 2). Along the gradient, mean annual air temperature ranged from 2.4°C to 10.0°C, and mean annual precipitation varied from 454 to 762 mm (Table 1). During and immediately preceding the period of record, all sites were relatively free from widespread forest disturbance that can supersede environmental controls on forest function (Amiro et al., 2010; Dore et al., 2012; Knowles et al., 2017). During the summer, the study area was variably influenced by the North American Monsoon, which increased with proximity to the core monsoon region in northwestern Mexico (Adams & Comrie, 1997). All sites received snow during the winter, but seasonal snow cover ranged from intermittent at lower latitudes/elevations to consistent seasonal cover at higher latitudes/elevations. Tree species composition was dominated by *Pinus ponderosa* at lower elevations and a mixture of *Pseudotsuga menziesii*, *Abies lasiocarpa*, and *Pinus contorta* at higher elevations (Table 1), stand age varied from approximately 80 to 120 years, and canopy height ranged from 10 to 18 m. In recognition of typically dry and wet periods during the warm season, we defined the following five seasons: winter (November–February), spring (March and April), pre-monsoon (May and June), monsoon (July and August), and fall (September and October).

### 2.2 | Data processing

We analyzed a total of 56 site-years of eddy covariance data from 1999 to 2018. Individual site data records ranged from 3 years (US-Vcs) to 20 years (US-NR1) and represented the complete site records in all cases except for US-Vcm that experienced a stand-replacing fire in 2013, after which data were excluded. All data were downloaded from the AmeriFlux network database (ameriflux.lbl.gov) as “BASE” 30 min data files that have undergone standardized

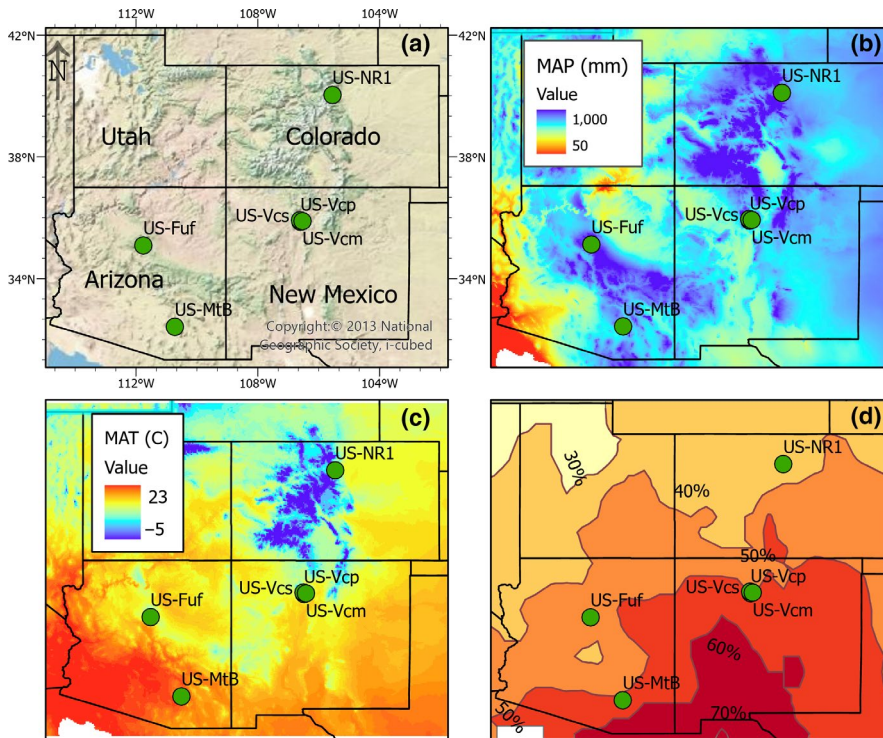


**FIGURE 1** Site map showing (a) the geographic locations of eddy covariance tower sites in the southwestern United States, (b) mean annual precipitation (MAP), (c) mean annual air temperature (MAT), and (d) monsoon (July and August) precipitation as a fraction of MAP for the period 1950–2000 ([www.worldclim.org](http://www.worldclim.org)). In this region, unusually steep moisture and air temperature gradients co-vary with elevation and proximity to the core monsoon precipitation region in northwestern Mexico [Colour figure can be viewed at [wileyonlinelibrary.com](http://wileyonlinelibrary.com)]

post-processing and quality assurance and control procedures. Evapotranspiration (ET) and net ecosystem exchange (NEE) fluxes were gapfilled using moving window “look-up” tables of ET or NEE under similar meteorological conditions in order to determine annual sums (Reichstein et al., 2005). These data were also subject to site-specific filters that identified and omitted periods of insufficient turbulent mixing based on the following threshold friction velocities: 0.20 m/s (US-Fuf), 0.22 m/s (US-Vcp), 0.40 m/s (US-MtB and US-NR1), 0.43 m/s (US-Vcs), and 0.52 m/s (US-Vcm). These values were either derived from the literature (US-Fuf: Dore et al., 2008; US-MtB: Knowles et al., 2020) or determined by the REdyProc algorithm (Wutzler et al., 2018) as the mean annual friction velocity threshold during the period of analysis. Direct NEE measurements were further partitioned into constituent GPP and ecosystem respiration ( $R_{eco}$ ) fluxes using both light-response curve and nighttime respiration algorithms (e.g., Figure 3; Lasslop et al., 2010; Reichstein et al., 2005); both approaches yielded similar results at all sites. Here, we present GPP data derived from the nighttime respiration method based on more accurate representation of midwinter vegetation dormancy (i.e.,  $GPP \approx 0$ ) at the coldest sites (Anderson-Teixeira, Delong, Fox, Brese, & Litvak, 2011; Monson et al., 2002). Observed meteorological data were not gapfilled.

## 2.3 | Statistical analysis

We tested the significance of leaf area index (LAI), air temperature ( $T_{air}$ ), vapor pressure deficit (VPD), and ET as predictors of seasonal and annual GPP using stepwise multiple regression analysis (Figure 4). We selected ET instead of precipitation as a proxy for

moisture availability because precipitation is subject to storage, runoff, and drainage, and because ET implicitly accounts for energy limitation that can decrease plant available water (Burns, Blanken, Turnipseed, Hu, & Monson, 2015; Scott & Biederman, 2019). This practice aligns with previous work supporting the use of ET as a metric to quantify the moisture available to vegetation at seasonal to annual timescales in semiarid systems (Biederman et al., 2017, 2018). In recognition of shared stomatal control over GPP and ET at short (i.e., diurnal) timescales, and the influence of  $T_{air}$  on saturation vapor pressure and VPD, we also considered the potential for evaporative fraction (EF; the ratio of the latent heat flux to the sum of the latent and sensible heat fluxes) to modify the relationship between  $T_{air}$  and GPP. Accordingly, site-specific half-hour data were used to establish seasonal linear relationships between  $T_{air}$  and GPP during non-light-limiting conditions (incoming solar radiation  $> 600 \text{ W/m}^2$ ;  $173 > n > 1,601$ ), and separate linear relationships above and below  $10^\circ\text{C}$  during the pre-monsoon. Significant ( $p < .05$ ) differences in the sensitivity of GPP to  $T_{air}$  between seasons, sites, and moisture regimes were subsequently determined using analysis of covariance; these sensitivities are discussed in the results section but not shown. After this analysis, the data were binned to facilitate visualization (Figure 5).

The mean LAI value for the 500 m pixel that contains each site was calculated from satellite-measured reflectance data (data retrieval period = 4 days) and obtained through the Oak Ridge National Laboratory Distributed Active Archive Center (Myneni, Knyazikhin, & Park, 2015). To account for coniferous physiology where stomata cover both sides of the needle leaf, two-sided LAI was generated by multiplying the one-sided MODIS LAI projection by two (Frank, Massman, Ewers, & Williams, 2019). For cross-site regressions,

seasonal or annual averages were calculated from the 4 day (LAI) or 30 min (all other variables) means and used as regression model inputs such that  $n = 56$  (56 site-years of data) for these analyses. Given that the MODIS LAI product is known to underestimate LAI in the presence of snow, especially for evergreen canopies (e.g., Tian et al., 2004), LAI was excluded from the winter analyses. In this way, iterative  $F$  tests were performed such that regression terms were sequentially included or excluded from the final models ( $p < .01$  in all cases) based on  $p$  value thresholds of 0.05 (inclusion) and 0.1 (exclusion), respectively. In other words, a predictor was entered into the stepwise model when the  $p$  value resultant from the one-predictor regression was below the significance threshold for inclusion ( $p < .05$ ). Similarly, whenever a new variable was added (i.e., to create a two or more variable predictor model), all candidate variables in the model were re-checked and excluded if their significance level was reduced above the specified significance threshold for exclusion ( $p > .1$ ). The resultant stepwise regression model forms were retained, standardized, and subsequently used to calculate the percent contribution of each significant predictor variable to the model's GPP prediction skill, expressed as the model  $R^2$  value (Lindeman, Merenda, & Gold, 1980). This analysis was performed using the "lmg" metric in the "relaimpo" package in the software R version 3.6.2 (Grömping, 2006). All other data analysis was performed using MATLAB version R2018a.

## 2.4 | Data analysis

All tower-based analyses were conducted using the 30 min data and the full multi-year records. From there, the data were smoothed or aggregated by site, season, or environmental conditions, in order to mitigate the possibility of data artifacts and to facilitate comparison among sites. GPP anomalies due to warming and drying were calculated by creating an "average" GPP month at each site and subtracting that from the GPP during the warmest or driest month on record at that site (Figure 6). This calculation was performed at the 30 min time step and then averaged to a mean daily value. For example, there were nine Januarys in the US-MtB dataset, each with 1,488 half-hour values. All nine Januarys were aligned, and the mean GPP was calculated at each time step such that each of the 1,488 "average" January GPP values represented the mean of nine data points from successive years. The "average" January was then subtracted from both the warmest and driest Januarys on record at US-MtB to determine the half-hourly GPP anomaly due to either warming or drying. These data were then averaged to daily (incoming solar radiation  $> 10 \text{ W/m}^2$ ) resolution ( $n = 31$  for January) and the month-specific daily anomalies were further grouped into high and low elevation categories and averaged to control for potentially different antecedent conditions among sites. Accordingly, each of the resulting boxplots (Figure 6) contains 28–31 (varies by month) daily data points that represent the average of the daily GPP anomaly due to either warming or drying at the three highest or lowest elevation sites.

## 3 | RESULTS

Precipitation distribution was influenced by elevation and proximity to the core region of the North American Monsoon such that the driest sites were located at low elevations near the geographic center of the study region (Figure 1; Table 1). In general, the variability of summer relative to winter precipitation increased with distance from the core monsoon region (not shown; Gutzler, 2004); the monsoon fraction of total annual precipitation specifically ranged from 46% at US-MtB ( $SD = 17\%$ ) to 20% ( $SD = 8\%$ ) at US-NR1 (Table 1). The seasonal variation of precipitation was larger at lower elevations and in areas more affected by the summer monsoon (Figure 2a), and the monsoon fraction of total annual precipitation was positively correlated with air temperature ( $p < .01$ ). Throughout the year,  $T_{\text{air}}$  followed a similar pattern at all sites with a peak during the monsoon season (Figure 2b). Based on the  $T_{\text{air}}$  range, US-MtB had the most moderate climate (seasonal  $T_{\text{air}}$  difference =  $13.4^\circ\text{C}$ ) and US-NR1 had the most extreme climate (seasonal  $T_{\text{air}}$  difference =  $18.7^\circ\text{C}$ ; Figure 2b). Among sites,  $T_{\text{air}}$  differences were greatest during the winter when mean  $T_{\text{air}}$  was above freezing at two sites (US-MtB and US-Fuf) and below freezing at four sites (US-Vcp, US-Vcs, US-Vcm, and US-NR1). Atmospheric demand for water, expressed as VPD, tracked  $T_{\text{air}}$  through the first half of the year before it was variably curtailed by the onset of summer monsoon precipitation and the associated rise in surface humidity (Figure 2c).

Despite the dominant evergreen vegetation, LAI varied between sites and to a lesser extent seasons (Figure 2d). Although seasonal LAI variability has been shown to result from changes in understory vegetation at some locations within the study area (White, Running, Nemani, Keane, & Ryan, 1997), the annual two-sided satellite-estimated LAI maxima were similar to reference ground-based LAI measurements at US-NR1 ( $4.0 \text{ m}^2/\text{m}^2$ ; Turnipseed, Blanken, Anderson, & Monson, 2002) and US-Fuf ( $2.3 \text{ m}^2/\text{m}^2$ ; Dore et al., 2008), and may indicate that LAI was systematically underestimated during the remainder of the year. This was particularly evident at US-NR1 where the seasonal LAI variability may have been exaggerated by periods of early or late snow cover (Heiskanen et al., 2012; Tian et al., 2004). Despite its relatively high elevation, peak LAI at US-Vcm was similar to the lowest elevation site (US-Fuf), and was likely suppressed by defoliation of the dominant tree species by the western spruce budworm (*Choristoneura freemani*; Dils et al., 2013). Annual ET ranged from 485 mm (US-Fuf) to 684 mm (US-MtB). Seasonally, maximum ET coincided with the summer monsoon period at all sites except US-Vcm where ET peaked during the pre-monsoon (Figure 2e). Among sites, seasonal GPP was greatest at either US-MtB (winter, spring, and fall) or US-NR1 (pre-monsoon and monsoon), which were the warmest and coldest sites, respectively (Figure 2f). Wintertime GPP ranged from near zero at the coldest sites to approximately 50% of the summer monthly maximum at the warmest US-MtB site. A transition occurred during the pre-monsoon and persisted throughout the monsoon where mean monthly GPP sharply increased at the highest elevation sites but leveled off everywhere else. The seasonal maximum GPP during the summer monsoon period at US-NR1 was 24% higher than the peak GPP at any other site.

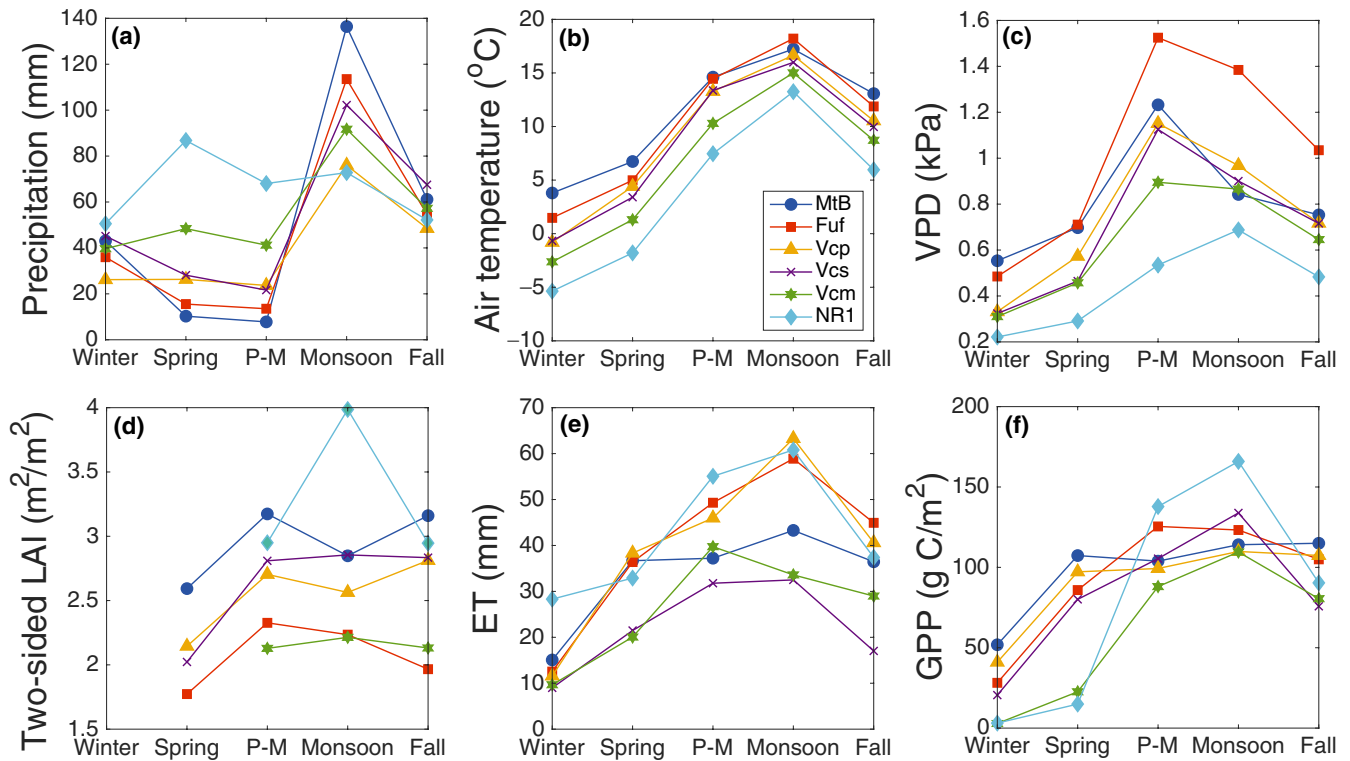


**FIGURE 2** Seasonal climatology, vegetation characteristics, and ecohydrological fluxes across the semiarid regional climatic gradient. The seasonal (a) precipitation, (b) air temperature, (c) vapor pressure deficit (VPD), (d) leaf area index (LAI), (e) evapotranspiration (ET), and (f) gross primary productivity (GPP) among sites. Winter (and spring at the two snowiest sites; US-NR1 and US-Vcm) LAI data are not shown due to problematic LAI retrievals during snow-covered periods. The air temperature, VPD, and LAI are seasonal averages; precipitation, ET, and GPP values are mean monthly sums. P-M is pre-monsoon [Colour figure can be viewed at [wileyonlinelibrary.com](http://wileyonlinelibrary.com)]

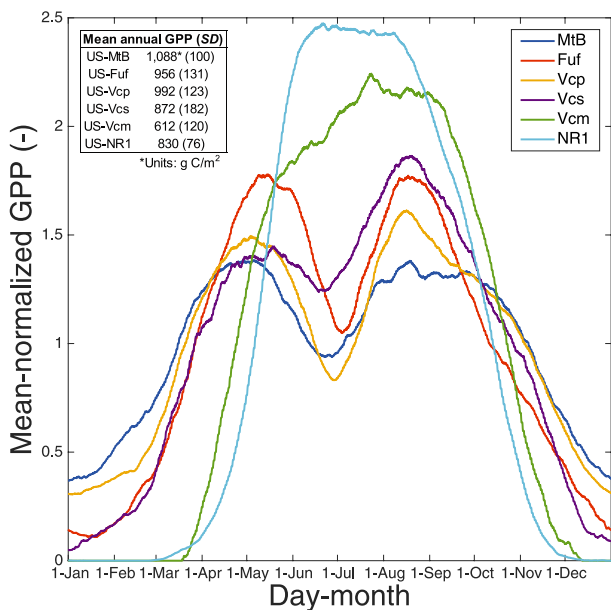


**FIGURE 3** Mean-normalized gross primary productivity (GPP) through time. Data are 30-day running means of half-hour values that have been normalized by the mean annual GPP at each site to emphasize the seasonality of vegetation activity. Inset shows the mean annual GPP during the period of record at each site. Ensemble averages range from 3 years (US-Vcs) to 20 years (US-NR1). SD is standard deviation [Colour figure can be viewed at [wileyonlinelibrary.com](http://wileyonlinelibrary.com)]

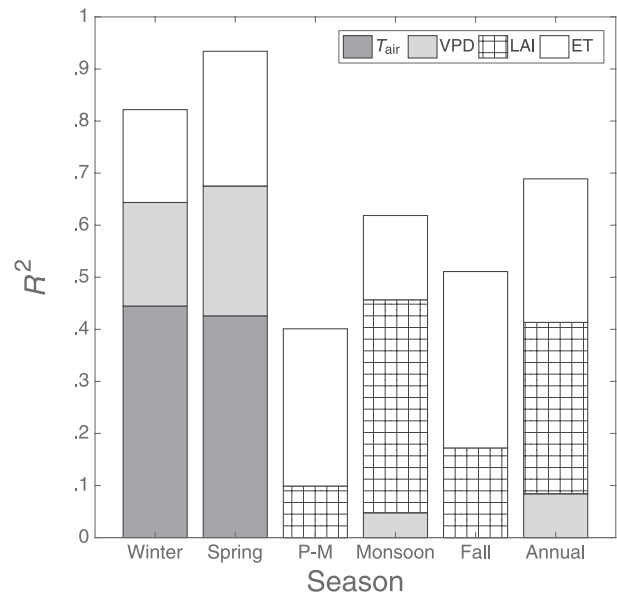


**FIGURE 4** The relative contribution of meteorological and ecohydrological predictor variables to the performance of cross-site gross primary productivity (GPP) models. Stepwise linear regression was used to isolate the significant ( $p < .05$ ) predictors of seasonal GPP. Significant model terms were then used to model the relative contribution of each predictor variable to whole-model R<sup>2</sup>. T<sub>air</sub>, VPD, and ET data were restricted to non-light-limiting (incoming solar radiation > 600 W/m<sup>2</sup>) conditions. P-M is pre-monsoon [Colour figure can be viewed at [wileyonlinelibrary.com](http://wileyonlinelibrary.com)]

Monthly fluxes normalized to each site's annual mean revealed three types of intra-annual GPP distributions (Figure 3): bimodal with higher GPP during the monsoon (US-Vcp and US-Vcs), bimodal with similar magnitude GPP peaks during the winter/spring and monsoon (US-MtB and US-Fuf), and unimodal with a broad peak during the warm season (US-Vcm and US-NR1). US-MtB and US-Vcp were the only sites that consistently maintained nonzero GPP throughout the winter, but relative GPP increases from winter to spring were also smallest at these sites (Figure 3). In contrast, the US-NR1 GPP increased rapidly from near zero to its annual maximum in only 3 months. During the pre-monsoon, there was a sharp GPP decrease at US-MtB, US-Fuf, and US-Vcp to approximately the mean annual value, less of a decrease at US-Vcs, and no pre-monsoon decrease at US-Vcm or US-NR1. The onset of monsoon precipitation brought increasing GPP at all sites with the exception of US-NR1 where precipitation was least during the monsoon season and GPP gradually declined. Similar to the spring transition (but opposite in sign), US-MtB and US-Vcp maintained post-monsoon peak GPP rates later into the season and the rate of GPP decrease in the fall was more gradual than at the other sites. Mean annual GPP ranged from 612 g C/m<sup>2</sup> at US-Vcm to 1,088 g C/m<sup>2</sup> at US-MtB (Figure 3 inset).

Relative importance modeling indicated a shift in the overarching controls on cross-site GPP from  $T_{\text{air}}$  in winter and spring, to

moisture availability (ET) in the pre-monsoon, to LAI during the monsoon (Figure 4). Similarities between the seasonal importance of VPD and  $T_{\text{air}}$  underscore the dependence of VPD on  $T_{\text{air}}$  via the saturation vapor pressure. LAI was a significant predictor of cross-site differences in GPP throughout the warm season (not considered during winter and spring due to problematic satellite retrievals; Tian et al., 2004), and especially during the monsoon when conditions were generally favorable to growth (Figure 4). Given the large contribution of monsoon GPP to the annual sum (Figure 2f), this effect carried over to the annual scale when LAI principally determined model performance, followed by moisture supply (ET) and demand (VPD).  $T_{\text{air}}$  did not contribute significantly to cross-site model performance at the annual scale, highlighting an overriding influence of moisture availability on GPP throughout the year. Indeed, ET was the only significant predictor of GPP during all seasons and for the entire year. Better model performance in the winter ( $R^2 = .82$ ), spring ( $R^2 = .93$ ), and monsoon ( $R^2 = .62$ ) seasons compared to the pre-monsoon ( $R^2 = .40$ ) and fall ( $R^2 = .51$ ) corresponds to periods of relatively similar and different limiting factors to cross-site GPP, respectively. In particular, the relative inability of this analysis to resolve pre-monsoon carbon cycling dynamics highlights the time-variant transition from cool season energy limitation to warm season moisture limitation across the regional climatic gradient.

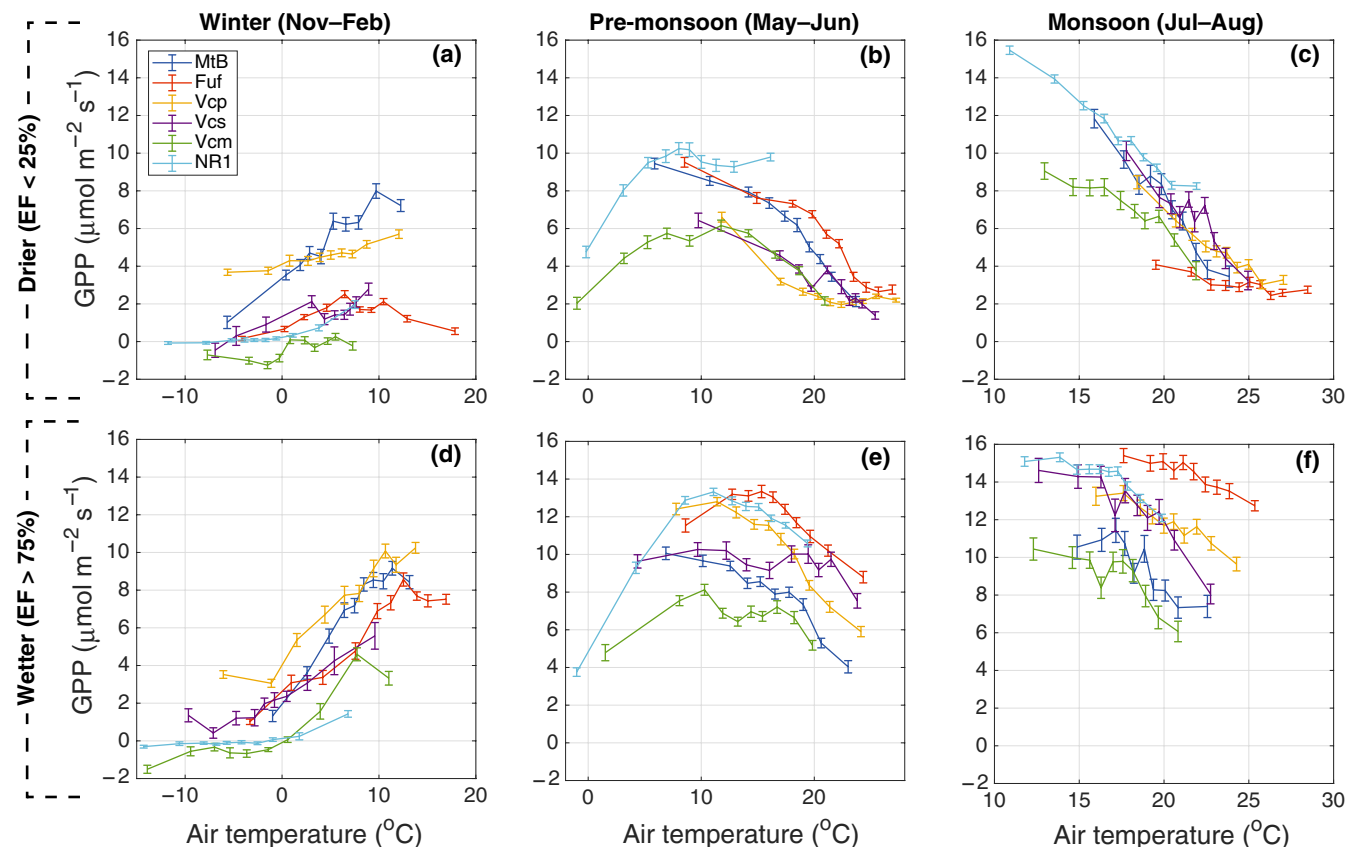


**FIGURE 5** Binned half-hour air temperature versus GPP during (a–c) seasonal periods of relative moisture limitation and (d–f) relative energy limitation as indicated by the evaporative fraction (EF), or the ratio of the latent heat flux to the sum of the latent and sensible heat fluxes. Data are restricted to non-light-limiting periods (incoming solar radiation > 600 W/m<sup>2</sup>). Bin sizes correspond to seasonal air temperature deciles and error bars denote the standard error. Note x-axis differences between panels [Colour figure can be viewed at [wileyonlinelibrary.com](http://wileyonlinelibrary.com)]

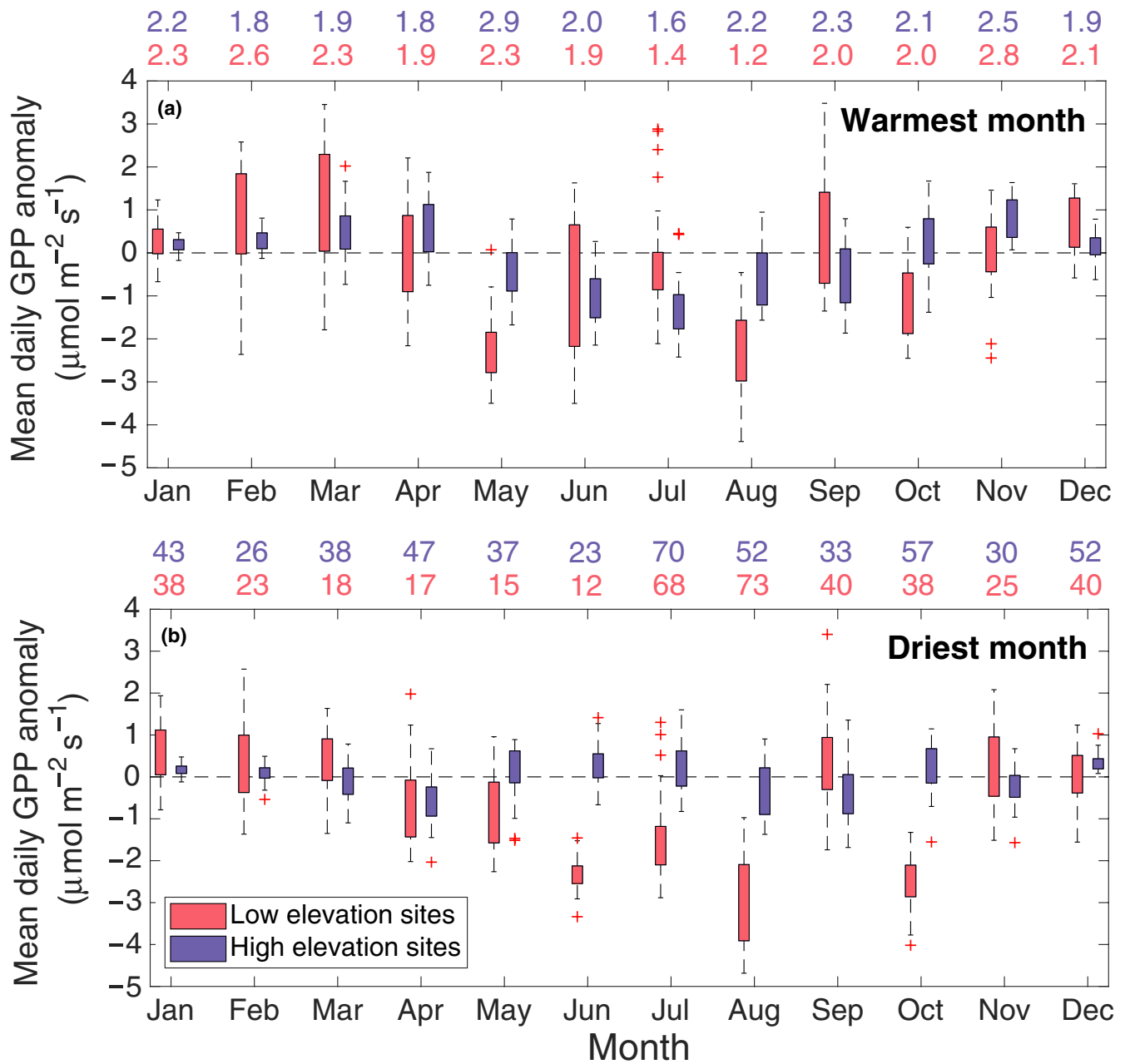


**FIGURE 6** Elevation-dependent gross primary productivity (GPP) differences between the (a) warmest and (b) driest months at each site relative to the average conditions. The low elevation sites are US-MtB, US-Fuf, and US-Vcp and the high elevation sites are US-Vcs, US-Vcm, and US-NR1 as shown in Table 1; data are daytime-only daily averages. For each box, the central mark is the median, the edges of the box are the 25th and 75th data percentiles, the whiskers extend to the most extreme data points not considered to be outliers by the MATLAB “boxplot” algorithm (default settings), and the outliers are plotted individually. The numbers above each panel correspond to the average (a) positive ( $^{\circ}\text{C}$ ) or (b) negative (mm) deviation from the mean during each of the warmest or driest months at the high (blue type) and low (red type) elevation sites [Colour figure can be viewed at [wileyonlinelibrary.com](http://wileyonlinelibrary.com)]

We used the EF to evaluate the relationship between air temperature and GPP during the driest ( $\text{EF} < 25\%$ ) and wettest ( $\text{EF} > 75\%$ ) seasonal periods at each site (Figure 5). During the winter, there was a positive relationship between  $T_{\text{air}}$  and GPP at all sites, and the addition of moisture significantly increased the GPP sensitivity to  $T_{\text{air}}$  (determined by analysis of covariance; see Section 2.3) everywhere but US-Vcs and US-NR1, the coldest site (Figure 5a,d). However, GPP was only sensitive to increasing  $T_{\text{air}}$  at US-NR1 during

periods of exceptionally warm weather before the onset of winter dormancy (data not shown); vegetation remained dormant throughout the mid-winter period. The pre-monsoon was a transition period whereby increasing  $T_{\text{air}}$  had a mixed effect on GPP with an inflection point near 10 degrees for the high elevation sites during dry conditions and for all sites during wet conditions (Figure 5b,e). For a given  $T_{\text{air}}$ , the pre-monsoon GPP was generally higher during periods of higher moisture, and pre-monsoon moisture also expanded

near-peak GPP fluxes to a broader  $T_{\text{air}}$  range. During the monsoon, all sites returned to a negative  $T_{\text{air}}$ -GPP relationship (Figure 5c,f). During periods of higher monsoon moisture, site-specific relationships between GPP and  $T_{\text{air}}$  developed at US-Fuf, US-Vcp, US-Vcs, and US-Vcm such that a given  $T_{\text{air}}$  resulted in a range of monsoon GPP values that decreased similarly with increasing  $T_{\text{air}}$ . Relative to these four sites, the wet monsoon GPP- $T_{\text{air}}$  relationship was significantly more negative at US-MtB (warmest site) and significantly less negative US-NR1 (coldest site), and US-MtB and US-NR1 were the only two sites where moisture significantly affected the monsoon GPP sensitivity to  $T_{\text{air}}$  (less negative with increasing moisture). In the absence of significant moisture limitation ( $EF > 75\%$ ), winter GPP peaked at 80% of the annual warm season maximum at US-MtB, 76% of the warm season maximum at US-Vcp, 56% at US-Fuf, 44% at US-Vcm, 38% at US-Vcs, and 9% at US-NR1 (Figure 5d,f).

To assess the potential impact of warming and drying scenarios on montane forest productivity from a global change perspective, we compared GPP from the warmest and driest instance of each calendar month during the multi-year records at each site to the site's average conditions (Figure 6). This analysis simulated an average of 2.1°C annual warming at both higher and lower elevation sites with 0.5°C greater summer (May–August) warming at higher compared to lower elevations and 0.4°C greater winter warming at lower compared to higher elevations (Figure 6a). Very high temperatures had a positive effect on cool season GPP and a negative effect on warm season GPP, and this pattern was amplified at lower elevation sites (Figure 6a). Relative to average conditions, the strongest positive  $T_{\text{air}}$  effect occurred in March at lower elevations and in April at higher elevations when snow melt moisture was typically abundant. A negative effect of extreme high  $T_{\text{air}}$  during the warm season was partially offset at lower elevations during the monsoon precipitation peak in July such that the maximum GPP reductions occurred in May and August; GPP reductions during high  $T_{\text{air}}$  conditions were roughly symmetrical throughout the warm season at the higher elevation sites. The driest instance of each calendar month corresponded to a monthly average precipitation deviation of 34 mm at lower elevations and 42 mm at higher elevations with the greatest monthly decrease during the monsoon at all sites (Figure 6b). Very dry weather had little impact on GPP at high elevations but did have a strong negative impact on warm season GPP at low elevations (Figure 6b). The GPP at lower elevations was negatively influenced by dry conditions beginning in April and May, and the magnitude of this effect roughly doubled from June to August, before variably subsiding throughout the fall. Small monthly GPP anomalies ( $<1 \mu\text{mol m}^{-2} \text{s}^{-1}$ ) throughout the year during dry conditions at the higher elevation sites demonstrate a relative insensitivity to drying.

## 4 | DISCUSSION

Montane forests are responsible for the majority of carbon sequestration in the western United States. Here, we identify intra-annual GPP distributions that result from variable but predictable

interactions among air temperature, moisture, and vegetation characteristics along a regional semiarid climatic gradient. Among sites, the maximum GPP occurred as a singular post-snow melt GPP peak at colder locations that also experienced near-complete winter dormancy. In contrast, GPP was sustained throughout the year at warmer sites, albeit with a distinctive foreshadowing depression, and these sites were stronger annual gross carbon sinks. Cross-site analysis indicated that LAI and moisture supply (ET) and demand (VPD) were significant predictors of total annual GPP, but  $T_{\text{air}}$  was not. However, there were signs that  $T_{\text{air}}$  indirectly affected GPP by regulating moisture availability, in particular a widespread trend toward increased cool season GPP and decreased warm season GPP during very warm periods. A companion analysis (Figure 6) also highlighted elevation as a first-order control on the sensitivity of GPP to extreme dry conditions. By considering multiple sites that span a broad climatic gradient, the current study identifies how regionally forecasted environmental changes are likely to affect semiarid montane forest carbon sequestration.

### 4.1 | Seasonal GPP distribution

In line with our prediction, we identified a shift from bimodal intra-annual GPP dynamics at lower elevations to unimodal intra-annual GPP dynamics at higher elevations with clear periods of vegetation activity and dormancy (Figure 3; Barnard et al., 2018). Taken together, this may indicate that vegetation has adapted to respond to the prevailing environmental conditions at each location (Martin et al., 2018; Roden & Ehleringer, 2007). Whereas abundant snow melt moisture stimulated the highest overall rates of warm season vegetation productivity (Figures 2f and 3), monsoon rains were critical to mid-summer vegetation recovery at the bimodal GPP sites characterized by foreshadowing drought (Figure 6b; Kolb, Dore, & Montes-Helu, 2013; Peltier & Ogle, 2019). These competing results reflect a variety of biophysical processes including deeper infiltration and storage of snow melt water in the soil profile where it can be accessed for a longer period of time (Fan et al., 2017; Hu et al., 2010), a “priming” effect of snow melt moisture on the persistence of fine root activity (Berkelhammer et al., 2020; Martin et al., 2018), and/or seasonal changes in atmospheric moisture demand (e.g., Novick et al., 2016). Given forecasted changes to both precipitation timing and type, the degree to which vegetation can continue to exploit seasonal water resources represents a key control on the persistence of the regional carbon sink (e.g., Grossiord et al., 2017).

### 4.2 | Temperature sensitivity of GPP

#### 4.2.1 | Cold season

The study sites spanned a gradient from typically winter active to typically winter dormant (Figures 2 and 3). In general, we found that warmer conditions translated to greater winter vegetation

activity. However, the temperature sensitivity of GPP was not uniform among sites and may have been inhibited by xylem blockage, decreased chlorophyll content, and/or other changes to the photosynthetic apparatus associated with winter hardening at the coldest sites (Figure 5; Bowling et al., 2018; Smith & Knapp, 1990). In contrast, photosynthetic acclimation, or changes in photosynthetic capacity with temperature, can occur more rapidly in warmer climates (Gea-Izquierdo et al., 2010; Nippert et al., 2004). It is therefore expected that minimum  $T_{\text{air}}$  thresholds for vegetation activity would vary among sites, and we specifically observed a range of winter  $T_{\text{air}}$  thresholds for non-light-limited photosynthetic activity from approximately 0°C at the coldest US-Vcm and US-NR1 sites to undefined (GPP > 0 at all times) at the warmest US-MtB site (Figure 5). In the absence of  $T_{\text{air}}$  limitation, potential GPP increased rapidly throughout the region, but was variably subject to moisture constraints that tempered the positive GPP response to warming (Figure 5). Near-perpetual daytime vegetation activity at US-MtB additionally supports that photoperiod can become a principal limitation to GPP in very mild winter climates (e.g., Kelly & Goulden, 2016). For context, mean winter photoperiod (incoming solar radiation > 10 W/m<sup>2</sup>) varied by ~40 min, or ~6% of mean winter daylength across the regional gradient. Overall, the presence of broad mechanistic similarities among sites signals that winter warming could stimulate regional GPP due to a combination of faster photosynthetic acclimation and higher photosynthetic capacity as air temperatures increase near the freezing point.

#### 4.2.2 | Warm season

A photosynthetic temperature optimum near 10°C was preserved through space and time (e.g., Huxman, Turnipseed, Sparks, Harley, & Monson, 2003; Figure 5). Given that mean  $T_{\text{air}}$  exceeded 10°C at all sites during the monsoon, and at the four lowest elevation sites during the pre-monsoon (Figure 2), warming had the effect of generally decreasing warm season GPP by decreasing the length of the optimal  $T_{\text{air}}$  time period. Exceptions to this occurred during periods of wet weather as a result of decreased VPD and enhanced stomatal conductance (Figure 5; Grossiord et al., 2020). We also observed a significant interaction between  $T_{\text{air}}$  and moisture where warming-induced monsoon GPP reductions were not as severe at both US-MtB and US-NR1 during relatively wet conditions. We found no evidence of substantial thermal acclimation to mean annual  $T_{\text{air}}$  (Niu et al., 2012), which suggests that (i) moisture constrains GPP more than  $T_{\text{air}}$  in these systems and (ii) the impacts of projected warming on GPP could be experienced similarly throughout the region. We did not, however, specifically consider the potential for species-level variations in leaf area, photosynthetic capacity, or resource use efficiency that can influence ecosystem carbon uptake (Monson et al., 2010; Nippert et al., 2004). Together, Figures 5 and 6 demonstrate a strong negative effect of summer warming on montane forest GPP and imply that the intra-annual GPP distribution may track temporal shifts in the photosynthetic

temperature optimum that is anticipated to occur both earlier in spring and later in fall.

### 4.3 | Environmental change impacts on semiarid montane forest carbon sequestration

Reduced snow accumulation in winter, also known as snow drought, is a robust climate change prediction in the western United States (Dierauer, Allen, & Whitfield, 2019; Harpold, Dettinger, & Rajagopal, 2017). Snow drought can result from drier and/or warmer (greater rain/snow ratio) winter conditions and has been linked to earlier snow melt and vegetation activity (Clow, 2010; Knowles et al., 2018). However, this scenario also accelerates soil moisture recession and ensuing vegetation moisture stress, which can lead to misalignment between the seasonal cycles of temperature and moisture availability during the critical early season carbon uptake period (Harpold et al., 2015; Monson et al., 2002; Winchell et al., 2016). Summer precipitation can compensate for snow water deficits, especially in areas affected by monsoon precipitation, but climate models have predicted future delays in the onset of the North American Monsoon (Cook & Seager, 2013; Grantz, Rajagopalan, Clark, & Zagona, 2007) and the potential for large reductions in monsoon precipitation (Pascale et al., 2017). Moreover, the timescales over which evergreen conifers may be capable of modifying their use of winter versus summer precipitation remain highly uncertain (Allen et al., 2019; Berkelhammer et al., 2020). To project the impact of forecasted climate change on montane forest GPP, the current study takes a synthetic approach that considers the potential for current cross-site biophysical relationships to parallel regional trends.

Climate extremes influence ecosystem structure and function through ecohydrological feedbacks that depend on the timing, extent, and type of disturbance (Sippel, Zscheischler, & Reichstein, 2016). A particularly relevant feedback, and an active research frontier in the western United States, concerns the potential for warming to trigger earlier vegetation greening, and to subsequently enhance early season ET at the expense of late season soil water availability (Buermann et al., 2018; Lian et al., 2020; Zhang, Parazoo, Williams, Zhou, & Gentine, 2020). In the current study, comparison of the warmest month at each site relative to average conditions simulated an average  $T_{\text{air}}$  increase of 2.1°C throughout the year, which is comparable to the magnitude of forecasted mid-century warming (2.1°C–2.7°C; Vose et al., 2017), and suggests that summer GPP deficits will be opposed by springtime GPP gains at both high and low elevations (Figure 6a). This type of compensatory response has been identified by a growing number of studies (Knowles et al., 2018; Wolf et al., 2016; Xu et al., 2020), and may herald good news for the persistence of the western United States carbon sink insofar as it counteracts increased respiration emissions with warming (e.g., Raich & Schlesinger, 1992). In contrast to the air temperature analysis, there was a clear effect of elevation on the regional GPP response to extreme dry conditions. Whereas

lower elevation (below ~2,500 m) forests were vulnerable to moisture limitation during the warm season, higher elevation (above ~2,700 m) forests remained insensitive to dry conditions throughout the year; winter GPP was generally robust to winter drying that is forecasted for semiarid western North America (Figure 6b; Jones & Gutzler, 2016). Hence, we conclude that the decadal carbon sequestration trajectory of the undisturbed semiarid montane forest biome will principally depend on the seasonality of warming insofar as it modulates ecosystem moisture availability via the physical and biological interactions described in this work. Given that these study sites were not heavily disturbed, we underscore that this conclusion does not account for threats to carbon sequestration from fire, biotic agents, and land-use change that are expected to increase and can result in vegetation shifts or deforestation with negative consequences for GPP (e.g., Anderegg et al., 2020; McDowell et al., 2020).

## 5 | CONCLUSION

We investigated seasonal interactions between air temperature, moisture, and vegetation within the context of montane forest productivity. We specifically characterize patterns of energy and water limitation across a semiarid climatic gradient that can be extrapolated to future conditions. Considering the distribution of GPP throughout the year, the current synthesis indicates a common trend toward longer tails (increased cool season productivity) and a bimodal shape (increased foresummer drought) with warming. This distribution is further subject to moisture limitation that can moderate the magnitude of both cool and warm season carbon gains, especially at lower elevations, but future patterns of monsoon precipitation remain highly uncertain. Consequently, the decadal magnitude of undisturbed montane forest carbon sequestration in the semiarid western United States will be modified by the counteracting feedbacks to expected climate warming and snow drought identified by this work.

## ACKNOWLEDGEMENTS

The US-MtB tower and associated data were supported by NSF awards EAR-1417101 and EAR-1331408. US-Vcp, US-Vcs, and US-Vcm were supported by U.S. Department of Energy (DOE) AmeriFlux Management Project subcontract number 7074628; US-NR1 was supported by DOE AmeriFlux Management Project subcontract number 7094866. J.F.K. was supported by the USDA and with funds from the DOE Office of Science. The authors wish to thank J. Chorover for managing the Santa Catalina Mountains & Jemez River Basin Critical Zone Observatory, which included the US-MtB, US-Vcp, US-Vcs, and US-Vcm sites, and R. Minor and N. Abramson (U. Arizona) for careful operation and maintenance of field instrumentation.

## DATA AVAILABILITY STATEMENT

The data that support the findings of this study are openly available from the AmeriFlux data repository at <https://ameriflux.lbl.gov>.

## ORCID

John F. Knowles  <https://orcid.org/0000-0002-3697-9439>

Joel A. Biederman  <https://orcid.org/0000-0002-1831-461X>

Sabina Dore  <https://orcid.org/0000-0003-2956-5251>

Marcy E. Litvak  <https://orcid.org/0000-0002-4255-2263>

## REFERENCES

- Adams, D. K., & Comrie, A. C. (1997). The North American monsoon. *Bulletin of the American Meteorological Society*, 78(10), 2197–2213. [https://doi.org/10.1175/1520-0477\(1997\)078<2197:TNAM>2.0.CO;2](https://doi.org/10.1175/1520-0477(1997)078<2197:TNAM>2.0.CO;2)
- Allen, S. T., Kirchner, J. W., Braun, S., Siegwolf, R. T. W., & Goldsmith, G. R. (2019). Seasonal origins of soil water used by trees. *Hydrology and Earth System Sciences*, 23(2), 1199–1210. <https://doi.org/10.5194/hess-23-1199-2019>
- Amiro, B. D., Barr, A. G., Barr, J. G., Black, T. A., Bracho, R., Brown, M., ... Xiao, J. (2010). Ecosystem carbon dioxide fluxes after disturbance in forests of North America. *Journal of Geophysical Research*, 115, G00K02. <https://doi.org/10.1029/2010JG001390>
- Anderegg, W. R. L., Trugman, A. T., Badgley, G., Anderson, C. M., Bartuska, A., Ciais, P., ... Randerson, J. (2020). Climate-driven risks to the climate mitigation potential of forests. *Science*, 368, eaaz7005. <https://doi.org/10.1126/science.aaz7005>
- Anderson-Teixeira, K. J., Delong, J. P., Fox, A. M., Brese, D. A., & Litvak, M. E. (2011). Differential responses of production and respiration to temperature and moisture drive the carbon balance across a climatic gradient in New Mexico. *Global Change Biology*, 17(1), 410–424. <https://doi.org/10.1111/j.1365-2486.2010.02269.x>
- Ault, T. R., Mankin, J. S., Cook, B. I., & Smerdon, J. E. (2016). Relative impacts of mitigation, temperature, and precipitation on 21st-century megadrought risk in the American Southwest. *Science Advances*, 2(10), e1600873. <https://doi.org/10.1126/sciadv.1600873>
- Baldocchi, D. D. (2020). How eddy covariance measurements have contributed to our understanding of Global Change Biology. *Global Change Biology*, 26(1), 242–260. <https://doi.org/10.1111/gcb.14807>
- Baldocchi, D. D., Finnigan, J., Wilson, K., Paw U, K. T., & Falge, E. (2000). On measuring net ecosystem carbon exchange over tall vegetation on complex terrain. *Boundary-Layer Meteorology*, 96(1/2), 257–291. <https://doi.org/10.1023/A:1002497616547>
- Barnard, D. M., Knowles, J. F., Barnard, H. R., Goulden, M. L., Hu, J., Litvak, M. E., & Molotch, N. P. (2018). Reevaluating growing season length controls on net ecosystem production in evergreen conifer forests. *Scientific Reports*, 8(1). <https://doi.org/10.1038/s41598-018-36065-0>
- Berkelhammer, M., Stefanescu, I. C., Joiner, J., & Anderson, L. (2017). High sensitivity of gross primary production in the Rocky Mountains to summer rain. *Geophysical Research Letters*, 44(8), 3643–3652. <https://doi.org/10.1002/2016GL072495>
- Berkelhammer, M., Still, C. J., Ritter, F., Winnick, M., Anderson, L., Carroll, R., ... Williams, K. H. (2020). Persistence and plasticity in conifer water-use strategies. *Journal of Geophysical Research: Biogeosciences*, 125(2). <https://doi.org/10.1029/2018JG004845>
- Biederman, J. A., Scott, R. L., Arnone III, J. A., Jasoni, R. L., Litvak, M. E., Moreo, M. T., ... Vivoni, E. R. (2018). Shrubland carbon sink depends upon winter water availability in the warm deserts of North America. *Agricultural and Forest Meteorology*, 249, 407–419. <https://doi.org/10.1016/j.agrformet.2017.11.005>
- Biederman, J. A., Scott, R. L., Bell, T. W., Bowling, D. R., Dore, S., Garatuzo-Payan, J., ... Goulden, M. L. (2017). CO<sub>2</sub> exchange and evapotranspiration across dryland ecosystems of southwestern North America. *Global Change Biology*, 23(10), 4204–4221. <https://doi.org/10.1111/gcb.13686>
- Boisvenue, C., & Running, S. W. (2010). Simulations show decreasing carbon stocks and potential for carbon emissions in Rocky Mountain

- forests over the next century. *Ecological Applications*, 20(5), 1302–1319. <https://doi.org/10.1890/09-0504.1>
- Bonan, G. B. (2008). Forests and climate change: Forcings, feedbacks, and the climate benefits of forests. *Science*, 320(5882), 1444–1449. <https://doi.org/10.1126/science.1155121>
- Bowling, D. R., Logan, B. A., Hufkens, K., Aubrecht, D. M., Richardson, A. D., Burns, S. P., ... Eiriksson, D. P. (2018). Limitations to winter and spring photosynthesis of a Rocky Mountain subalpine forest. *Agricultural and Forest Meteorology*, 252, 241–255. <https://doi.org/10.1016/j.agrformet.2018.01.025>
- Brooks, P. D., & Vivoni, E. R. (2008). Mountain ecohydrology: Quantifying the role of vegetation in the water balance of montane catchments. *Ecohydrology*, 1(3), 187–192. <https://doi.org/10.1002/eco.27>
- Buermann, W., Forkel, M., O'Sullivan, M., Stith, S., Friedlingstein, P., Haverd, V., ... Richardson, A. D. (2018). Widespread seasonal compensation effects of spring warming on northern plant productivity. *Nature*, 562(7725), 110–114. <https://doi.org/10.1038/s41586-018-0555-7>
- Burns, S. P., Blanken, P. D., Turnipseed, A. A., Hu, J., & Monson, R. K. (2015). The influence of warm-season precipitation on the diel cycle of the surface energy balance and carbon dioxide at a Colorado subalpine forest site. *Biogeosciences*, 12(23), 7349–7377. <https://doi.org/10.5194/bg-12-7349-2015>
- Charney, N. D., Babst, F., Poulter, B., Record, S., Trouet, V. M., Frank, D., ... Evans, M. E. K. (2016). Observed forest sensitivity to climate implies large changes in 21st century North American forest growth. *Ecology Letters*, 19(9), 1119–1128. <https://doi.org/10.1111/ele.12650>
- Clow, D. W. (2010). Changes in the timing of snowmelt and streamflow in Colorado: A response to recent warming. *Journal of Climate*, 23(9), 2293–2306. <https://doi.org/10.1175/2009JCLI2951.1>
- Cook, B. I., & Seager, R. (2013). The response of the North American Monsoon to increased greenhouse gas forcing. *Journal of Geophysical Research: Atmospheres*, 118(4), 1690–1699. <https://doi.org/10.1002/jgrd.50111>
- Davis, K. T., Dobrowski, S. Z., Higuera, P. E., Holden, Z. A., Veblen, T. T., Rother, M. T., ... Maneta, M. P. (2019). Wildfires and climate change push low-elevation forests across a critical climate threshold for tree regeneration. *Proceedings of the National Academy of Sciences of the United States of America*, 116(13), 6193–6198. <https://doi.org/10.1073/pnas.1815107116>
- Dierauer, J. R., Allen, D. M., & Whitfield, P. H. (2019). Snow drought risk and susceptibility in the western United States and southwestern Canada. *Water Resources Research*, 55(4), 3076–3091. <https://doi.org/10.1029/2018WR023229>
- Dils, C., Boyd, C., White, A., Anhold, J., Fairweather, M. L., Grady, A., ... Dudley, S. (2013). *Forest insect and disease conditions in the southwestern region, 2013* (PR-R3-16-12; Southwestern Region Forest Health, p. 43). Washington, DC: United States Department of Agriculture.
- Dore, S., Kolb, T. E., Montes-Helu, M., Sullivan, B. W., Winslow, W. D., Hart, S. C., ... Hungate, B. A. (2008). Long-term impact of a stand-replacing fire on ecosystem CO<sub>2</sub> exchange of a ponderosa pine forest. *Global Change Biology*, 14(8), 1801–1820. <https://doi.org/10.1111/j.1365-2486.2008.01613.x>
- Dore, S., Montes-Helu, M., Hart, S. C., Hungate, B. A., Koch, G. W., Moon, J. B., ... Kolb, T. E. (2012). Recovery of ponderosa pine ecosystem carbon and water fluxes from thinning and stand-replacing fire. *Global Change Biology*, 18(10), 3171–3185. <https://doi.org/10.1111/j.1365-2486.2012.02775.x>
- Fan, Y., Miguez-Macho, G., Jobbágy, E. G., Jackson, R. B., & Otero-Casal, C. (2017). Hydrologic regulation of plant rooting depth. *Proceedings of the National Academy of Sciences of the United States of America*, 114(40), 10572–10577. <https://doi.org/10.1073/pnas.1712381114>
- Frank, J. M., Massman, W. J., Ewers, B. E., & Williams, D. G. (2019). Bayesian analysis of 17 winters of water vapor fluxes show bark beetles reduce sublimation. *Water Resources Research*, 55, 1598–1623. <https://doi.org/10.1029/2018WR023054>
- Gea-Izquierdo, G., Mäkelä, A., Margolis, H., Bergeron, Y., Black, T. A., Dunn, A., ... Berninger, F. (2010). Modeling acclimation of photosynthesis to temperature in evergreen conifer forests. *New Phytologist*, 188, 175–186. <https://doi.org/10.1111/j.1469-8137.2010.03367.x>
- Grantz, K., Rajagopalan, B., Clark, M., & Zagana, E. (2007). Seasonal shifts in the North American monsoon. *Journal of Climate*, 20(9), 1923–1935. <https://doi.org/10.1175/JCLI4091.1>
- Griscom, B. W., Adams, J., Ellis, P. W., Houghton, R. A., Lomax, G., Miteva, D. A., ... Fargione, J. (2017). Natural climate solutions. *Proceedings of the National Academy of Sciences of the United States of America*, 114(44), 11645–11650. <https://doi.org/10.1073/pnas.1710465114>
- Grömping, U. (2006). Relative importance for linear regression in R: The package relaimpo. *Journal of Statistical Software*, 17(1). <https://doi.org/10.18637/jss.v017.i01>
- Grossiord, C., Buckley, T., Cernusak, L. A., Novick, K. A., Poulter, B., Siegwolf, R. T. W., ... McDowell, N. G. (2020). Plant responses to rising vapor pressure deficit. *New Phytologist*, 226(6), 1550–1566. <https://doi.org/10.1111/nph.16485>
- Grossiord, C., Sevanto, S., Dawson, T. E., Adams, H. D., Collins, A. D., Dickman, L. T., ... McDowell, N. G. (2017). Warming combined with more extreme precipitation regimes modifies the water sources used by trees. *New Phytologist*, 213(2), 584–596. <https://doi.org/10.1111/nph.14192>
- Gutzler, D. S. (2004). An index of interannual precipitation variability in the core of the North American Monsoon region. *Journal of Climate*, 17(22), 4473–4480. <https://doi.org/10.1175/3226.1>
- Harpold, A., Brooks, P., Rajagopal, S., Heidebuchel, I., Jardine, A., & Stielstra, C. (2012). Changes in snowpack accumulation and ablation in the intermountain west. *Water Resources Research*, 48(11), W11501. <https://doi.org/10.1029/2012WR011949>
- Harpold, A., Dettinger, M., & Rajagopal, S. (2017). Defining snow drought and why it matters. *Eos*. <https://doi.org/10.1029/2017EO068775>
- Harpold, A. A., Molotch, N. P., Musselman, K. N., Bales, R. C., Kirchner, P. B., Litvak, M., & Brooks, P. D. (2015). Soil moisture response to snowmelt timing in mixed-conifer subalpine forests. *Hydrological Processes*, 29(12), 2782–2798. <https://doi.org/10.1002/hyp.10400>
- Havranek, W., & Tranquillini, W. (1995). Physiological processes during winter dormancy and their ecological significance. In W. K. Smith & T. M. Hinckley (Eds.), *Ecophysiology of coniferous forests* (pp. 95–124). San Diego, CA: Academic Press.
- Heiskanen, J., Rautiainen, M., Stenberg, P., Möttöus, M., Vesanto, V.-H., Korhonen, L., & Majasalmi, T. (2012). Seasonal variation in MODIS LAI for a boreal forest area in Finland. *Remote Sensing of Environment*, 126, 104–115. <https://doi.org/10.1016/j.rse.2012.08.001>
- Hessburg, P. F., Miller, C. L., Parks, S. A., Povak, N. A., Taylor, A. H., Higuera, P. E., ... Salter, R. B. (2019). Climate, environment, and disturbance history govern resilience of western North American forests. *Frontiers in Ecology and Evolution*, 7. <https://doi.org/10.3389/fevo.2019.00239>
- Hu, J., Moore, D. J. P., Burns, S. P., & Monson, R. K. (2010). Longer growing seasons lead to less carbon sequestration by a subalpine forest. *Global Change Biology*, 16(2), 771–783. <https://doi.org/10.1111/j.1365-2486.2009.01967.x>
- Huxman, T. E., Turnipseed, A. A., Sparks, J. P., Harley, P. C., & Monson, R. K. (2003). Temperature as a control over ecosystem CO<sub>2</sub> fluxes in a high-elevation, subalpine forest. *Oecologia*, 134(4), 537–546. <https://doi.org/10.1007/s00442-002-1131-1>
- Jones, S. M., & Gutzler, D. S. (2016). Spatial and seasonal variations in aridification across southwest North America. *Journal of Climate*, 29, 4637–4649. <https://doi.org/10.1175/JCLI-D-14-00852.1>
- Keeling, C. D., Chin, J. F. S., & Whorf, T. P. (1996). Increased activity of northern vegetation inferred from atmospheric CO<sub>2</sub> measurements. *Nature*, 382, 146–149. <https://doi.org/10.1038/382146a0>

- Kelly, A. E., & Goulden, M. L. (2016). A montane Mediterranean climate supports year-round photosynthesis and high forest biomass. *Tree Physiology*, 36(4), 459–468. <https://doi.org/10.1093/treephys/tpv131>
- Knowles, J. F., Lestak, L. R., & Molotch, N. P. (2017). On the use of a snow aridity index to predict remotely sensed forest productivity in the presence of bark beetle disturbance. *Water Resources Research*, 53(6), 4891–4906. <https://doi.org/10.1002/2016WR019887>
- Knowles, J. F., Molotch, N. P., Trujillo, E., & Litvak, M. E. (2018). Snowmelt-driven trade-offs between early and late season productivity negatively impact forest carbon uptake during drought. *Geophysical Research Letters*, 45(7), 3087–3096. <https://doi.org/10.1002/2017GL076504>
- Knowles, J. F., Scott, R. L., Minor, R. L., & Barron-Gafford, G. A. (2020). Ecosystem carbon and water cycling from a sky island montane forest. *Agricultural and Forest Meteorology*, 281, 107835. <https://doi.org/10.1016/j.agrformet.2019.107835>
- Kolb, T., Dore, S., & Montes-Helu, M. (2013). Extreme late-summer drought causes neutral annual carbon balance in southwestern ponderosa pine forests and grasslands. *Environmental Research Letters*, 8(1), 015015. <https://doi.org/10.1088/1748-9326/8/1/015015>
- Lasslop, G., Reichstein, M., Papale, D., Richardson, A. D., Arneeth, A., Barr, A., ... Wohlfahrt, G. (2010). Separation of net ecosystem exchange into assimilation and respiration using a light response curve approach: Critical issues and global evaluation. *Global Change Biology*, 16(1), 187–208. <https://doi.org/10.1111/j.1365-2486.2009.02041.x>
- Lian, X., Piao, S., Li, L. Z. X., Li, Y., Huntingford, C., Ciais, P., ... McVicar, T. R. (2020). Summer soil drying exacerbated by earlier spring greening of northern vegetation. *Science Advances*, 6(1), eaax0255. <https://doi.org/10.1126/sciadv.aax0255>
- Lindeman, R. H., Merenda, P. F., & Gold, R. Z. (1980). *Introduction to bivariate and multivariate analysis*. Glenview, IL: Scott, Foresman and Company.
- Litvak, M. (2016). *AmeriFlux US-Vcs valles caldera sulphur springs mixed conifer, dataset*. <https://doi.org/10.17190/AMF/1418681>
- Luce, C. H., Vose, J. M., Pederson, N., Campbell, J., Millar, C., Kormos, P., & Woods, R. (2016). Contributing factors for drought in United States forest ecosystems under projected future climates and their uncertainty. *Forest Ecology and Management*, 380(C), 299–308. <https://doi.org/10.1016/j.foreco.2016.05.020>
- Martin, J., Looker, N., Hoylman, Z., Jencso, K., & Hu, J. (2018). Differential use of winter precipitation by upper and lower elevation Douglas fir in the Northern Rockies. *Global Change Biology*, 24(12), 5607–5621. <https://doi.org/10.1111/gcb.14435>
- McDowell, N. G., Allen, C. D., Anderson-Teixeira, K., Aukema, B. H., Bond-Lamberty, B., Chini, L., ... Xu, C. (2020). Pervasive shifts in forest dynamics in a changing world. *Science*, 368, eaaz9463. <https://doi.org/10.1126/science.aaz9463>
- Millar, C. I., & Stephenson, N. L. (2015). Temperate forest health in an era of emerging megadisturbance. *Science*, 349(6250), 823–826. <https://doi.org/10.1126/science.aaa9933>
- Monson, R. K., Prater, M. R., Hu, J., Burns, S. P., Sparks, J. P., Sparks, K. L., & Scott-Denton, L. E. (2010). Tree species effects on ecosystem water-use efficiency in a high-elevation, subalpine forest. *Oecologia*, 162(2), 491–504. <https://doi.org/10.1007/s00442-009-1465-z>
- Monson, R. K., Turnipseed, A. A., Sparks, J. P., Harley, P. C., Scott, D., Sparks, K. L., & Huxman, T. E. (2002). Carbon sequestration in a high-elevation, subalpine forest. *Global Change Biology*, 8, 459–478. <https://doi.org/10.1046/j.1365-2486.2002.00480.x>
- Myneni, R., Knyazikhin, Y., & Park, T. (2015). MCD15A3H MODIS/Terra+Aqua leaf area index/FPAR 4-day L4 global 500m SIN grid V006. NASA EOSDIS land processes DAAC. <https://doi.org/10.5067/MODIS/MCD15A3H.006>
- Nippert, J. B., Duursma, R. A., & Marshall, J. D. (2004). Seasonal variation in photosynthetic capacity of montane conifers. *Functional Ecology*, 18(6), 876–886. <https://doi.org/10.1111/j.0269-8463.2004.00909.x>
- Niu, S., Luo, Y., Fei, S., Yuan, W., Schimel, D., Law, B. E., ... Zhou, X. (2012). Thermal optimality of net ecosystem exchange of carbon dioxide and underlying mechanisms. *New Phytologist*, 194(3), 775–783. <https://doi.org/10.1111/j.1469-8137.2012.04095.x>
- Novick, K. A., Ficklin, D. L., Stoy, P. C., Williams, C. A., Bohrer, G., Oishi, A. C., ... Phillips, R. P. (2016). The increasing importance of atmospheric demand for ecosystem water and carbon fluxes. *Nature Climate Change*, 6(11), 1023–1027. <https://doi.org/10.1038/nclimate3114>
- Pan, Y., Birdsey, R. A., Fang, J., Houghton, R., Kauppi, P. E., Kurz, W. A., ... Hayes, D. (2011). A large and persistent carbon sink in the world's forests. *Science*, 333(6045), 988–993. <https://doi.org/10.1126/science.1201609>
- Pascale, S., Boos, W. R., Bordoni, S., Delworth, T. L., Kapnick, S. B., Murakami, H., ... Zhang, W. (2017). Weakening of the North American monsoon with global warming. *Nature Climate Change*, 7, 806–812. <https://doi.org/10.1038/NCLIMATE3412>
- Pase, C. P., & Brown, D. E. (1994). Rocky Mountain (Petran) and Madrean Montane conifer forests. In D. E. Brown (Ed.), *Biotic communities: Southwestern United States and northwestern Mexico* (pp. 43–48). Salt Lake City, UT: University of Utah Press.
- Peltier, D. M. P., & Ogle, K. (2019). Legacies of La Niña: North American monsoon can rescue trees from winter drought. *Global Change Biology*, 25(1), 121–133. <https://doi.org/10.1111/gcb.14487>
- Petersky, R. S., Shoemaker, K. T., Weisberg, P. J., & Harpold, A. A. (2019). The sensitivity of snow ephemerality to warming climate across an arid to montane vegetation gradient. *Ecohydrology*, 12(2), e2060. <https://doi.org/10.1002/eco.2060>
- Potts, D. L., Minor, R. L., Braun, Z., & Barron-Gafford, G. A. (2017). Photosynthetic phenological variation may promote coexistence among co-dominant tree species in a Madrean sky island mixed conifer forest. *Tree Physiology*, 37(9), 1229–1238. <https://doi.org/10.1093/treephys/tpx076>
- Raich, J. W., & Schlesinger, W. H. (1992). The global carbon dioxide flux in soil respiration and its relationship to vegetation and climate. *Tellus Series B*, 44(2), 81–89. <https://doi.org/10.1034/j.1600-0889.1992.t01-1-00001.x>
- Reichstein, M., Falge, E., Baldocchi, D., Papale, D., Aubinet, M., Berbigier, P., ... Valentini, R. (2005). On the separation of net ecosystem exchange into assimilation and ecosystem respiration: Review and improved algorithm. *Global Change Biology*, 11, 1424–1439. <https://doi.org/10.1111/j.1365-2486.2005.001002.x>
- Reyes-Fox, M., Steltzer, H., Trlica, M. J., McMaster, G. S., Andales, A. A., LeCain, D. R., & Morgan, J. A. (2014). Elevated CO<sub>2</sub> further lengthens growing season under warming conditions. *Nature*, 510(7504), 259–262. <https://doi.org/10.1038/nature13207>
- Roden, J. S., & Ehleringer, J. R. (2007). Summer precipitation influences the stable oxygen and carbon isotopic composition of tree-ring cellulose in *Pinus ponderosa*. *Tree Physiology*, 27(4), 491–501. <https://doi.org/10.1093/treephys/27.4.491>
- Schimel, D., Kittel, T. G. F., Running, S., Monson, R., Turnipseed, A., & Anderson, D. (2002). Carbon sequestration studied in western U.S. mountains. *Eos, Transactions American Geophysical Union*, 83(40), 445. <https://doi.org/10.1029/2002EO000314>
- Schwalm, C. R., Williams, C. A., Schaefer, K., Baldocchi, D., Black, T. A., Goldstein, A. H., ... Scott, R. L. (2012). Reduction in carbon uptake during turn of the century drought in western North America. *Nature Geoscience*, 5(8), 551–556. <https://doi.org/10.1038/ngeo1529>
- Scott, R. L., & Biederman, J. A. (2019). Critical zone water balance over 13 years in a semiarid savanna. *Water Resources Research*, 55(1), 574–588. <https://doi.org/10.1029/2018WR023477>
- Sippel, S., Zscheischler, J., & Reichstein, M. (2016). Ecosystem impacts of climate extremes crucially depend on the timing. *Proceedings of the National Academy of Sciences of the United States of America*, 113(21), 5768–5770. <https://doi.org/10.1073/pnas.1605667113>
- Sloat, L. L., Henderson, A. N., Lamanna, C., & Enquist, B. J. (2015). The effect of the foresummer drought on carbon exchange in subalpine

- meadows. *Ecosystems*, 18(3), 533–545. <https://doi.org/10.1007/s10021-015-9845-1>
- Smith, W. K., & Knapp, A. K. (1990). Ecophysiology of high elevation forests. In W. D. Billings, F. Golley, O. L. Lange, J. S. Olson, & H. Remmert (Eds.), *Plant biology of the basin and range* (Vol. 80, pp. 87–142). Berlin and Heidelberg, Germany: Springer. [https://doi.org/10.1007/978-3-642-74799-1\\_4](https://doi.org/10.1007/978-3-642-74799-1_4)
- Sun, J., Oncley, S. P., Burns, S. P., Stephens, B. B., Lenschow, D. H., Campos, T., ... Coons, T. (2010). A multiscale and multidisciplinary investigation of ecosystem-atmosphere CO<sub>2</sub> exchange over the Rocky Mountains of Colorado. *Bulletin of the American Meteorological Society*, 91(2), 209–230. <https://doi.org/10.1175/2009BAMS2733.1>
- Szejner, P., Wright, W. E., Babst, F., Belmecheri, S., Trouet, V., Leavitt, S. W., ... Monson, R. K. (2016). Latitudinal gradients in tree ring stable carbon and oxygen isotopes reveal differential climate influences of the North American Monsoon System. *Journal of Geophysical Research: Biogeosciences*, 121(7), 1978–1991. <https://doi.org/10.1002/2016JG003460>
- Tian, Y., Dickinson, R. E., Zhou, L., Zeng, X., Dai, Y., Myneni, R. B., ... Shaikh, M. (2004). Comparison of seasonal and spatial variations of leaf area index and fraction of absorbed photosynthetically active radiation from Moderate Resolution Imaging Spectroradiometer (MODIS) and Common Land Model. *Journal of Geophysical Research*, 109(D1), D01103. <https://doi.org/10.1029/2003JD003777>
- Trujillo, E., Molotch, N. P., Goulden, M. L., Kelly, A. E., & Bales, R. C. (2012). Elevation-dependent influence of snow accumulation on forest greening. *Nature Geoscience*, 5(10), 705–709. <https://doi.org/10.1038/ngeo1571>
- Turnipseed, A. A., Blanken, P. D., Anderson, D. E., & Monson, R. K. (2002). Energy budget above a high-elevation subalpine forest in complex topography. *Agricultural and Forest Meteorology*, 110(3), 177–201. [https://doi.org/10.1016/S0168-1923\(01\)00290-8](https://doi.org/10.1016/S0168-1923(01)00290-8)
- Vose, R. S., Easterling, D. R., Kunkel, K. E., LeGrande, A. N., & Wehner, M. F. (2017). Temperature changes in the United States. In D. J. Wuebbles, D. W. Fahey, K. A. Hibbard, D. J. Dokken, B. C. Stewart, & T. K. Maycock (Eds.), *Climate science special report: Fourth national climate assessment* (Vol. 1, pp. 185–206). Washington, DC: U.S. Global Change Research Program. <https://doi.org/10.7930/JON29V45>
- White, J. D., Running, S. W., Nemani, R., Keane, R. E., & Ryan, K. C. (1997). Measurement and remote sensing of LAI in Rocky Mountain montane ecosystems. *Canadian Journal of Forest Research*, 27, 1714–1727. <https://doi.org/10.1139/x97-142>
- Wieser, G. (1997). Carbon dioxide gas exchange of cembran pine (*Pinus cembra*) at the alpine timberline during winter. *Tree Physiology*, 17(7), 473–477. <https://doi.org/10.1093/treephys/17.7.473>
- Williams, A. P., Allen, C. D., Macalady, A. K., Griffin, D., Woodhouse, C. A., Meko, D. M., ... McDowell, N. G. (2013). Temperature as a potent driver of regional forest drought stress and tree mortality. *Nature Climate Change*, 3(3), 292–297. <https://doi.org/10.1038/nclimate1693>
- Winchell, T. S., Barnard, D. M., Monson, R. K., Burns, S. P., & Molotch, N. P. (2016). Earlier snowmelt reduces atmospheric carbon uptake in midlatitude subalpine forests. *Geophysical Research Letters*, 43(15), 8160–8168. <https://doi.org/10.1002/2016GL069769>
- Wolf, S., Keenan, T. F., Fisher, J. B., Baldocchi, D. D., Desai, A. R., Richardson, A. D., ... van der Laan-Luijkx, I. T. (2016). Warm spring reduced carbon cycle impact of the 2012 US summer drought. *Proceedings of the National Academy of Sciences of the United States of America*, 113(21), 5880–5885. <https://doi.org/10.1073/pnas.1519620113>
- Wutzler, T., Lucas-Moffat, A., Migliavacca, M., Knauer, J., Sickel, K., Šigut, L., ... Reichstein, M. (2018). Basic and extensible post-processing of eddy covariance flux data with REdDyProc. *Biogeosciences*, 15(16), 5015–5030. <https://doi.org/10.5194/bg-15-5015-2018>
- Xu, B., Arain, M. A., Black, T. A., Law, B. E., Pastorello, G. Z., & Chu, H. (2020). Seasonal variability of forest sensitivity to heat and drought stresses: A synthesis based on carbon fluxes from North American forest ecosystems. *Global Change Biology*, 26(2), 901–918. <https://doi.org/10.1111/gcb.14843>
- Zhang, Y., Parazoo, N. C., Williams, A. P., Zhou, S., & Gentine, P. (2020). Large and projected strengthening moisture limitation on end-of-season photosynthesis. *Proceedings of the National Academy of Sciences of the United States of America*, 117(17), 9216–9222. <https://doi.org/10.1073/pnas.1914436117>

**How to cite this article:** Knowles JF, Scott RL, Biederman JA, et al. Montane forest productivity across a semiarid climatic gradient. *Glob Change Biol*. 2020;26:6945–6958. <https://doi.org/10.1111/gcb.15335>